SF2A 2019
P. Di Matteo, O. Creevey, A. Crida, G. Kordopatis, J. Malzac, J.-B. Marquette, M. N'Diaye, O. Venot (eds)

DETECTION OF INTRA-CLUSTER DIFFUSE LIGHT: PRESENTING DAWIS

A. Ellien[1], F. Durret[1] and C. Adami[2]

Abstract. We present our new wavelet package, `DAWIS`, developped to detect intra-cluster light (ICL), the optical diffuse component of galaxy clusters. We use it to investigate the properties of a massive galaxy cluster at $z \sim 0.5$, MACS J0717.5+3745, and of its extended filament. Using *Hubble* Frontier Fields* (HFF) data in the F105W, F814W, F606W, and F435W filters, we compute the ICL fractions in the core of MACS J0717.5+3745, and find large contributions of ICL, a result that is consistent with other studies.

Keywords: Image processing, Galaxies, Galaxy clusters, Photometry

1 Introduction

Since the first mention by Zwicky (1951) of a very diffuse and extended halo of light around the central galaxy of the Coma cluster, the so-called ICL has been a growing field of research in astronomy. We now believe that it is composed of stars which are not gravitationally bound to any galaxy in particular, but are rather bound to the global gravitational potential of a galaxy cluster. While the presence of ICL in galaxy clusters is no longer questioned, its formation mechanisms are still a matter of debate, whether it is due to violent galaxy-galaxy interactions (Mihos 2004), to tidal stripping (Byrd & Valtonen 1990) or to star formation (Sommer-Larsen 2006).
The ICL is a very low-surface-brightness source, and its detection is a tricky task, due to the various instrumental effects (point spread function, scattered light, flat-fielding error...), the need for deep photometric data, and contamination by other astronomical features (bright foreground stars, galaxtic cirrus). Various methods have been used to perform this analysis, such as galaxy light profile fitting (Jiménez-Teja & Dupke 2016)), raw masking of sources (Montes & Trujillo 2018) or wavelet analysis (Da Rocha et al. 2008). Here we chose a wavelet analysis approach and created `DAWIS`, a Detection Algorithm with Wavelets for Intra-cluster light Surveys which is parallelized and optimized to run on large images.

2 `DAWIS` in a nutshell

`DAWIS` is based on Mallat's *à trous* wavelet algorithm (Shensa 1992), which is particularly suited for astronomical images. It is a fast, discrete, redundant wavelet transform that respects flux conservation. By applying this algorithm, an image is convolved in $N_{\rm lvl}$ wavelet planes, following a multi-scale vision as described in Bijaoui & Rué (1995). The process is done by iteratively smoothing the original image $N_{\rm lvl} + 1$ times with a varying B-spline kernel, the difference between two successive smoothed images giving a wavelet plane. Each wavelet plane contains features with a characteristic size of 2^n pixels, n being the index of the plane ($n = 0, 1, 2, 3, ..., N_{\rm lvl}$). Small values of n correspond to bright and compact luminous features, while greater values correspond to large and low-intensity ones, with $n = N_{\rm lvl}$ corresponding to the large sky background variations.
After the wavelet convolution, astronomical objects are decomposed into several features through the different wavelet planes. In each plane, we apply a thresholding to determine the statistically significant pixels composing these features. The detection threshold is estimated in each wavelet plane separately: a standard deviation of the intensity, σ_n, is computed using a 3σ clipping algorithm, and the significant pixels are set to have intensity

[1] Sorbonne Université, CNRS, UMR 7095, Institut d'Astrophysique de Paris, 98bis Bd Arago, F-75014 Paris
[2] Aix-Marseille Univ., CNRS, CNES, LAM, Marseille, France
*`https://archive.stsci.edu/pub/hlsp/frontier/`

© Société Francaise d'Astronomie et d'Astrophysique (SF2A) 2019

Table 1. Detection thresholds and ICL fractions computed for each of the four filters of the HFF. The thresholds are used to create the ICL maps from the residual images (see Fig. 2). The fractions are computed from the ICL maps and the reconstructed images in the four filters within the radius that is indicated for each filter. Error bars correspond to the 95% confidence intervals. The radii are the same as in Jiménez-Teja et al. (2019) for comparison purposes.

HFF	F435W	F606W	F814W	F105W
$3\sigma_{\rm bkg}$ (mag.arcsec^{-2})	29.89	29.96	30.03	29.97
$5\sigma_{\rm bkg}$ (mag.arcsec^{-2})	29.34	29.41	29.50	29.41
Radius (kpc)	275.3	562.5	421.5	FoV
$f_{\rm ICL}(\%)$	$2.48^{+0.19}_{-0.20}$	$24.43^{+3.37}_{-1.71}$	$16.10^{+1.03}_{-1.03}$	$13.22^{+1.76}_{-1.49}$

values higher than $k\sigma_n$. This threshold is different for each wavelet plane, but the same value k is applied everywhere.
After thresholding, the significant pixels are grouped in regions using scale-by-scale segmentation. We then create inter-scale trees by linking together significant regions from different planes by looking at their spatial distribution. Trees with connected regions from at least three different planes are recognized as valid representations of astronomical objects in the wavelet space. The objects are then reconstructed using a conjugate gradient algorithm (Starck et al. 1998).

3 ICL in MACS J0717.5+3745

After pre-processing (binning, point spread function deconvolution, masking of foreground sources, see Ellien et al. (2019) for more details), we apply `DAWIS` to images from the HFF in four bands: F105W, F814W, F606W, and F435W. For each image we detect and reconstruct all the galaxies (see Figure 1), and then create residual images by subtracting all those features from the original one (see Figure 2). We then detect ICL in the residual images by computing a detection threshold $\sigma_{\rm bkg}$ from the sky background (see Table 1). The ICL fractions are computed using the following formula

$$f_{\rm ICL} = \frac{F_{\rm ICL}}{F_{\rm gal} + F_{\rm ICL}}, \tag{3.1}$$

where $F_{\rm ICL}$ is the integrated flux of ICL and $F_{\rm gal}$ is the integrated flux of MACS J0717.5+3745's galaxies. $F_{\rm ICL}$ is obtained by summing the pixel values with values greater than $3\sigma_{\rm bkg}$ in the ICL maps, and $F_{\rm gal}$ is obtained by summing the pixel values of the cluster's galaxy profiles in the reconstructed images. The errors on the ICL fraction are computed with a bootstrap on the values of the pixels of the galaxies and of the pixels of the ICL. For each filter, we create a sample with all the pixels belonging to Red Sequence galaxies of the reconstructed image, and a sample with all the ICL pixels of the residual image. We draw $N = 10000$ sub-samples randomly from each sample, allowing the same pixel value to be drawn multiple times. We then compute the given ICL fraction for each sub-sample which gives N values of ICL fractions for each filter. The errors on the true ICL fraction value are then estimated by computing a 95% confidence interval on the sub-sample values.

4 Conclusions

Our resulting ICL fractions (see Table 1) are coherent with previous studies such as Jiménez-Teja et al. (2019) where they find ICL fractions (in %) of 7.22 ± 0.81 in the F435W, 22.27 ± 3.68 in the F606W and 13.63 ± 3.60 in the F814W. This showcases `DAWIS` ability to detect and reconstruct galaxies in an image up to high precision. We find that there is almost no ICL in the F435W filter (UV rest frame), indicating that there is little star formation in the ICL. The ICL fraction seems to peak in the F606W before slowly decreasing as it gets redder. In parallel, we tried to detect intra-filament light (IFL) in the extended cosmic filament associated to MACS J0717.5+3745 using the same analysis method but in a different *Hubble* Space Telescope mosaic, without success. More informations about the core of MACSJ 0717.5+3745 and a study of its extended filament can be found in Ellien et al. (2019).

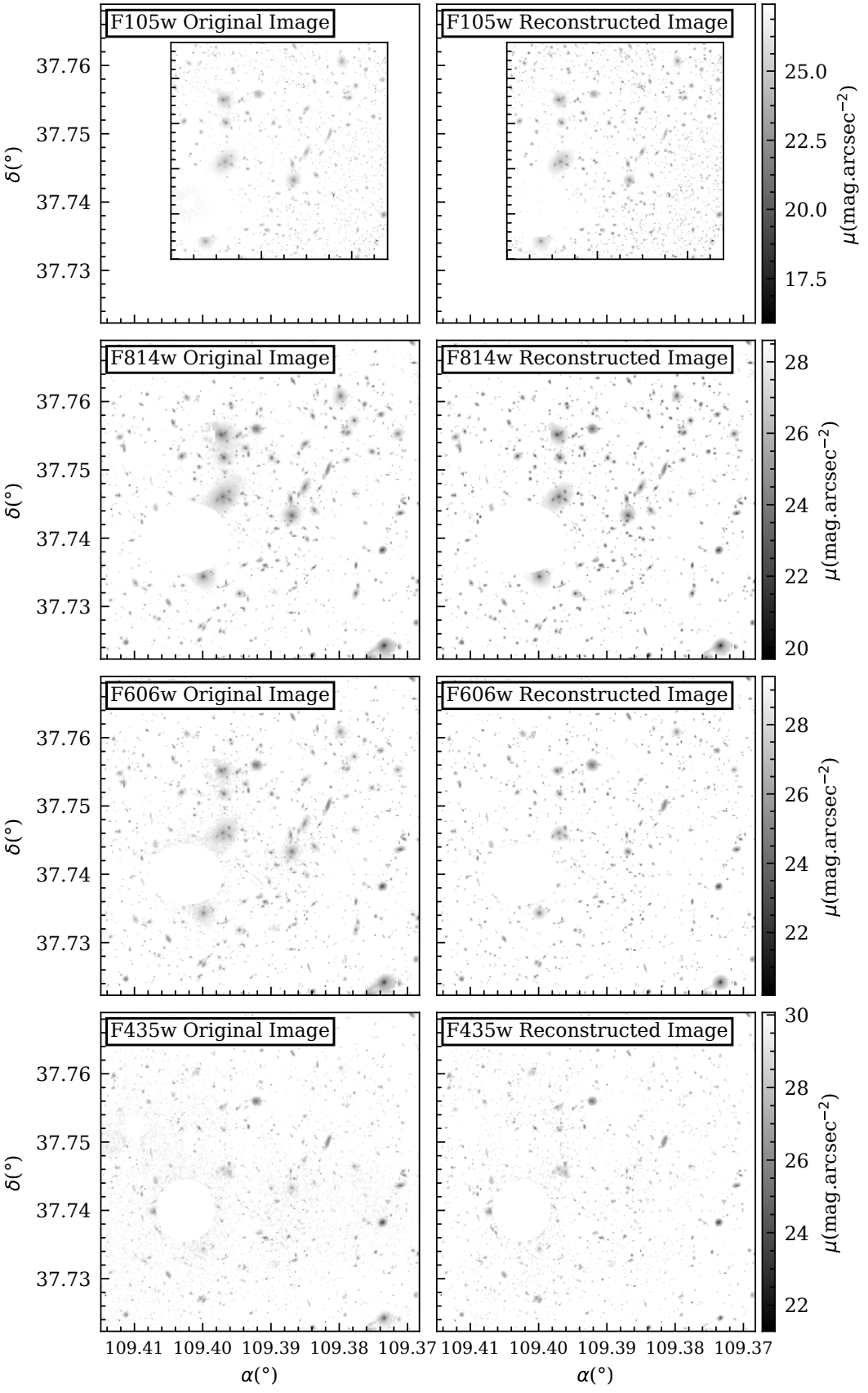

Fig. 1. Left column: original HFF images in the four filters after PSF deconvolution and masking of star residuals and of the large foreground galaxy. Right column: stacked images of objects detected and reconstructed by three runs of `DAWIS`.

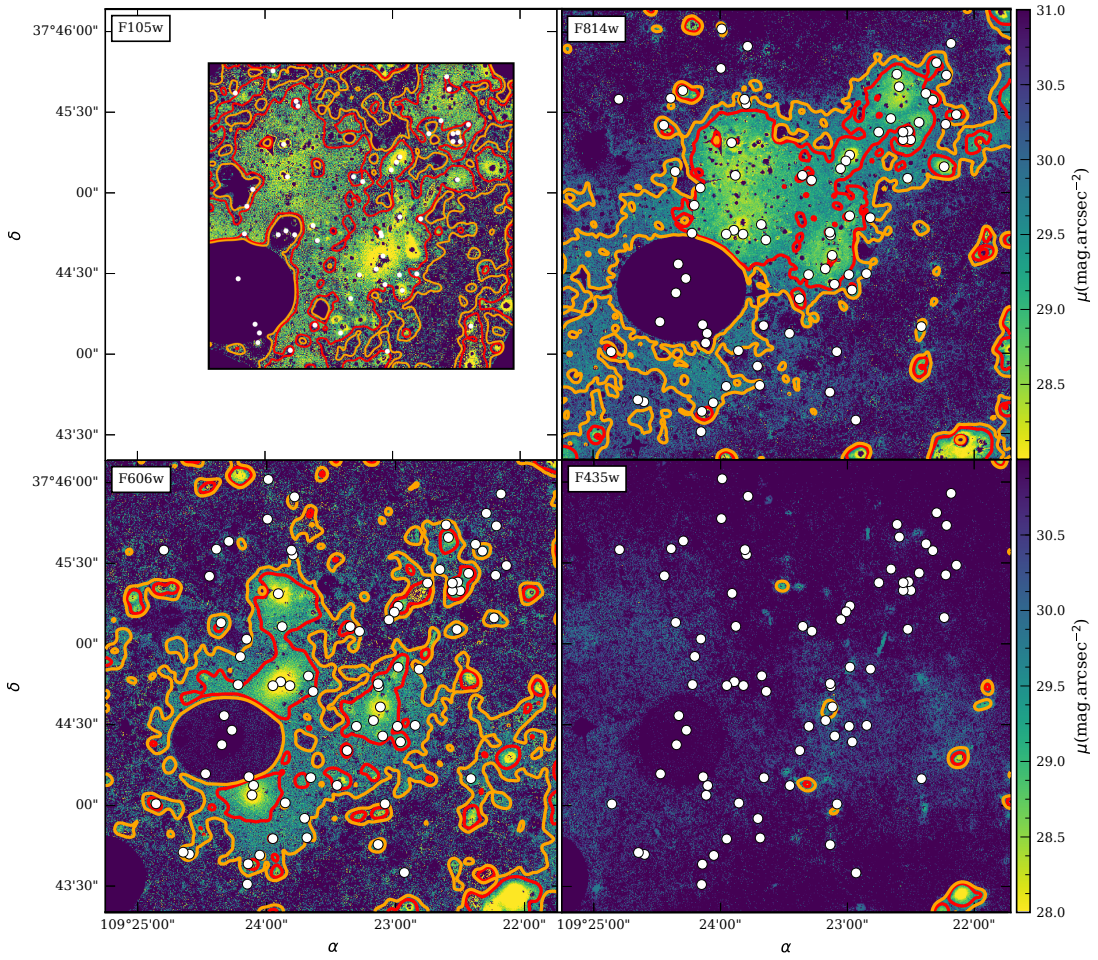

Fig. 2. Surface brightness maps of the residuals after wavelet processing by `DAWIS` in each band. The orange contours show $3\sigma_{\rm bkg}$ detection and the red ones $5\sigma_{\rm bkg}$. The white dots show the galaxies in the cluster redshift range ($0.53 < z < 0.56$). From top to bottom and left to right: F435W, F606W, F814W, and F105W. The contours are smoothed with a Gaussian kernel of $\sigma = 5$ for the map to be readable.

References

Bijaoui, A. & Rué, F. 1995, Signal Processing, 46, 345

Byrd, G. & Valtonen, M. 1990, ApJ, 350, 89

Da Rocha, C., Ziegler, B. L., & Mendes de Oliveira, C. 2008, MNRAS, 388, 1433

Ellien, A., Durret, F., Adami, C., et al. 2019, A&A, 628, A34

Jiménez-Teja, Y. & Dupke, R. 2016, ApJ, 820, 49

Jiménez-Teja, Y., Dupke, R. A., Lopes de Oliveira, R., et al. 2019, A&A, 622, A183

Mihos, J. C. 2004, in IAU Symposium, Vol. 217, Recycling Intergalactic and Interstellar Matter, ed. P.-A. Duc, J. Braine, & E. Brinks, 390

Montes, M. & Trujillo, I. 2018, MNRAS, 474, 917

Shensa, M. J. 1992, IEEE Trans. Signal Processing, 40, 2464

Sommer-Larsen, J. 2006, MNRAS, 369, 958

Starck, J.-L., Murtagh, F. D., & Bijaoui, A. 1998, Image Processing and Data Analysis, 297

Zwicky, F. 1951, PASP, 63, 61